Elastic Scattering of 14-MeV Neutrons by Deuterons*

A. C. Berick,† R. A. J. Riddle, and C. M. York
Physics Department, University of California, Los Angeles, California 90024
(Received 25 January 1968)

The differential cross section for the elastic scattering of neutrons by deuterons was measured at a neutron energy of 14.3±0.2 MeV. The data cover the center-of-mass scattering angles from 13.5° to 158.6°, and the cross section at each angle was measured with a statistical accuracy from 2 to 3%. The scattering sample was a deuterated benzene scintillator coupled to a photomultiplier tube. The time of flight of the scattered neutron was measured by utilizing the recoil-deuteron pulse in the scattering-sample counter to start the timer, and a pulse produced by the scattered neutron in a plastic scintillation counter to stop it. Background events were limited by placing pulse-height restrictions on the pulses from the scattering-sample counter. The data were normalized to the experimentally determined *n-p* scattering cross section at 14.1 MeV. The relative efficiency of the scattered-neutron detector at each energy was determined by performing the experiment with a nondeuterated benzene scintillator in place of the deuterated target. The angles chosen for the *n-p* scattering were those for which the neutron energies were the same as those for the scattering angles chosen for the *n-d* experiment. The known values of the *n-p* scattering cross section were then used to evaluate the *n-d* cross section. The angular distribution shows a deeper minimum near 120° and higher values in the forward directions than is indicated by previous experimental results. An eighth-order polynomial is required to fit the angular distribution, and the value of the total cross section is in good agreement with earlier values.

I. INTRODUCTION

THE nucleon-deuteron interaction has been intensively studied[1–8] in the hope of obtaining information about the nature of the forces between nucleons. Comparisons of *p-d* and *n-d* elastic scattering could give information on the charge symmetric nature of these forces, while studies of the inelastic interactions could shed light on the *n-n* interaction. Based on the work thus far completed, it is clear that a combination of very precise measurements and equally precise methods of theoretical analysis are required to obtain this desired information.

The measurement of the elastic *n-d* scattering at 14 MeV reported here was undertaken to provide accurate data for small angles of scattering. These data would then complement the work on *p-d* elastic scattering in this energy region.[5] The use of modern neutron time-of-flight measuring techniques together with precise angular resolution has made it possible to achieve a set of data on the elastic *n-d* process which is far more accurate than any previously reported in this energy region.

* Work supported by the National Science Foundation.
† National Science Foundation Predoctoral Fellow; present address: Los Alamos Scientific Laboratory, Los Alamos, N. M.

[1] J. C. Allred, A. H. Armstrong, and L. Rosen, Phys. Rev. **91**, 90 (1953); J. D. Seagrave, *ibid.* **97**, 757 (1955).
[2] H. S. W. Massey, *Progress in Nuclear Physics* (Pergamon Press, London, 1953), pp. 235–270.
[3] R. S. Christian and J. L. Gammel, Phys. Rev. **91**, 100 (1953).
[4] L. D. Fadeev, Zh. Eksperim. i Teor. Fiz. **39**, 1459 (1960) [English transl.: Soviet Phys.—JETP **12**, 1014 (1961)]; R. Aaron, R. D. Amado, and Y. Y. Yam, Phys. Rev. **140**, B1291 (1965); **136**, B650 (1964); V. S. Bhasin, G. L. Schrenk, and A. N. Mitra, *ibid.* **137**, B398 (1965); A. C. Phillips, *ibid.* **142**, 984 (1966).
[5] As an example, see S. K. Kuchi, J. Sanada, S. Suwa, I. Hayashi, K. Nisimura, and K. Fukunaga, J. Phys. Soc. Japan **15**, 9 (1960).
[6] B. E. Bonner, thesis, Rice University, 1965 (unpublished); J. D. Seagrave, and J. C. Hopkins (to be published).
[7] M. D. Goldberg, V. M. May, and J. R. Stehn, Brookhaven National Laboratory Report No. BNL-400, 1962 (unpublished).
[8] A. C. Berick, Ph.D. thesis, UCLA, 1967 (unpublished).

II. EXPERIMENTAL METHOD

A beam of 14-MeV neutrons was allowed to strike a scintillation counter filled with deuterated benzene. The recoiling deuterons, produced in a neutron-deuteron collision, could be detected in this scattering-sample scintillator. The scattered neutrons were then detected in a plastic disk of scintillator some distance away and their times of flight measured electronically. In addition to the neutron time of flight, a pulse-height analysis on the recoiling deuteron was performed to improve the selection of true elastic scattering events from the background events. The experimental set up is indicated in Fig. 1.

The differential cross section can be written in terms of the experimentally measured parameters as

$$\frac{d\sigma_{nd}}{d\Omega}(\theta)=\frac{C_{nd}(\theta)}{\epsilon(E_{nd})N_d I_0}, \qquad (1)$$

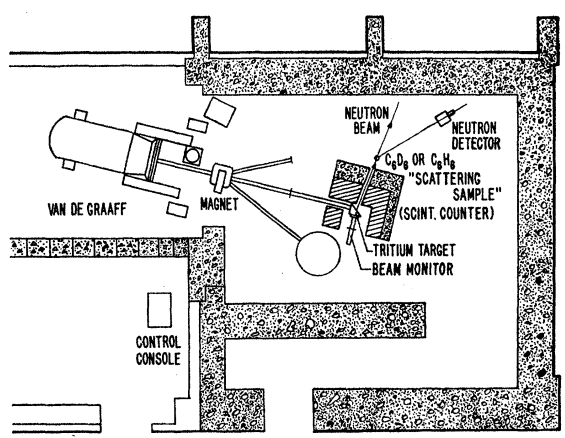

FIG. 1. Plan view of the experimental area.

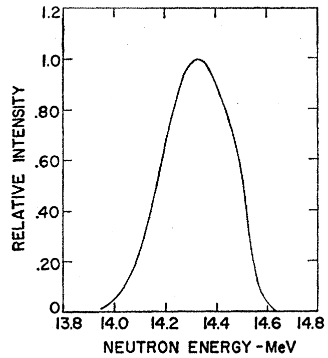

FIG. 2. Calculated energy distribution of neutron beam.

where $C_{nd}(\theta)$ is the number of valid scattering events recorded with the detector at the laboratory angle θ, $\epsilon(E_{nd})$ is the efficiency of the apparatus for detecting neutrons of energy E_{nd}, E_{nd} is the energy of a neutron, with incident energy E_0, after being elastically scattered from a deuteron through the angle θ, I_0 is the flux of monoenergetic neutrons incident on the scattering sample during the time in which C_{nd} events were recorded, and N_d is the number of deuterons in the scattering sample.

In the present experiment I_0 was not measured directly. In its place a quantity called M was recorded, where M is the number of recoil α particles from the $T(d,n)He^4$ reaction recorded by a thin plastic scintillation counter placed at right angles to the deuteron beam, as shown in Fig. 1. M is proportional to I_0. N_d was determined by a chemical analysis of the scattering sample, and $\epsilon(E_{nd})$ was determined by performing an n-p scattering experiment analogous to that performed for the n-d determination. In this case the scattering sample was an ordinary nondeuterated benzene scintillator identical in composition to the deuterated sample. The n-p differential cross section can be written in the form

$$\frac{d\sigma_{np}}{d\Omega}(\theta')=\frac{C_{np}(\theta')}{\epsilon'(E_{np})N_p I_0'}, \tag{2}$$

where the terms are completely analogous to those in Eq. (1). For each value of θ there is a θ' for which $E_{np}=E_{nd}$. For these angles $\epsilon'=\epsilon$, since the detection efficiency is a function of energy only. Furthermore, if the number of beam monitor counts M is the same for each measurement, then $I_0'=I_0$. Now if Eqs. (1) and (2) are combined, one obtains

$$\frac{d\sigma_{nd}}{d\Omega}(\theta)=\frac{d\sigma_{np}}{d\Omega}(\theta')\frac{N_p}{N_d}\frac{C_{nd}(\theta)}{C_{np}(\theta')}. \tag{3}$$

Thus the n-d differential cross section at 14 MeV is expressed in terms of experimentally determined quantities. The n-p cross section at 14 MeV has been determined in other experiments.[1,9]

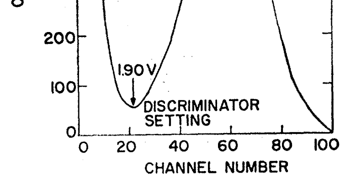

FIG. 3. Pulse-height spectrum produced in the monitor counter by recoiling α particles.

III. APPARATUS

A. Neutron Beam

Monoenergetic neutrons of 14 MeV were obtained from the $T(d,n)He^4$ reaction. The UCLA 2-MeV Van de Graaff accelerator, shown in Fig. 1, was used to produce a deuteron beam which was incident upon a tritium target. The minimum energy to which deuterons could be accelerated while maintaining stable beam currents was 500 keV. This has an accelerator-associated limitation which had to be used even though 500 keV is somewhat above the energy corresponding to the peak of the cross section for neutron production and is such as to introduce some kinematic spread in the beam energy. The energy spread of the neutron beam was calculated[8] and the results are shown in Fig. 2. The mean energy of the distribution coincides with the most probable energy and the distribution is given by $14.33_{-0.16}^{+0.18}$ MeV, where the limits are taken from the points at half-maximum.

B. Counters

The liquid scintillators used as scattering samples (NE230 and NE231) were obtained from Nuclear Enterprises, Ltd., of Winnipeg, Canada. The scintillator was supplied in cylindrical aluminum bubble-free cells, with an active liquid volume 2 in. in height and 2 in. in diameter. The inner surfaces of the aluminum cells were coated with titanium oxide, which forms a diffuse, white reflecting surface. From the data supplied by the manufacturer[10] it was possible to determine the ratio $N_p/N_d = 1.0124$, which is needed in Eq. (3).

[9] H. H. Barschall and R. F. Taschek, Phys. Rev. **75**, 1819 (1949).
[10] P. Leggate (private communication).

The recoil α-particle detector was used as a beam monitor and consisted of a 56 AVP photomultiplier tube with a disk of NE102 plastic scintillator, 0.25 in. in diameter and 0.005 in. thick, cemented to the photocathode. The tritium target holder was equipped with a moveable aluminum "flap" which could be rotated remotely to block the α particles emanating from the target in the direction of the detector in order to measure background effects. The α particles striking the detector under normal conditions were not monoenergetic but did have a reasonably well-defined energy, as seen in the pulse-height spectrum of Fig. 3. By setting the discriminator threshold at 1.90 V as indicated in the figure, the α-to-background counting ratio was maximized and the sensitivity of the detected counts to small shifts of the photomultiplier gain was minimized. The result was a very stable beam monitoring device.

The neutron detector consisted of a 58 AVP photomultiplier tube with a cylinder of plastic scintillator, 4.5 in. in diameter and 2.0 in. high, mounted on its photocathode. The neutron-detection threshold for this detector was set at approximately 2.5 MeV for the forward scattering laboratory angles from 10° to 65° and at approximately 0.5 MeV for the backward angles from 70° to 140°.

C. Electronic Circuitry

A portion of the data was taken utilizing a two-parameter analysis, where neutron time of flight was displayed against scattering-sample counter pulse height, while the remaining data were taken with a one-dimensional time-of-flight display in which valid scattering-sample counter pulses were restricted with respect to pulse height by a single-channel analyzer. Figure 4(a) is an electronic block diagram of the former setup while Fig. 4(b) is a block diagram for the latter. The circuits indicated in these diagrams are of a conventional nature or have been described in detail elsewhere.[11]

The circuits were tested daily with the aid of a mercury switch pulser to determine that all of the logic functions were being performed properly, that discriminator thresholds had not drifted, that the pulse-height analysis was responding in a linear fashion, and that the time-of-flight system was in calibration. The discriminator thresholds were held constant to within 0.05 V during the experiment. The gain of the photomultipliers was checked periodically by irradiating them with a Na^{22} source and observing the position of the Compton scattering edge for the 1.28-MeV γ rays. The deuterated benzene of the scattering-sample counter had a 5% greater light output than the regular benzene, but the tube voltage was adjusted to give equal responses while performing the n-p portion of the experiment. The measurements at different angles required

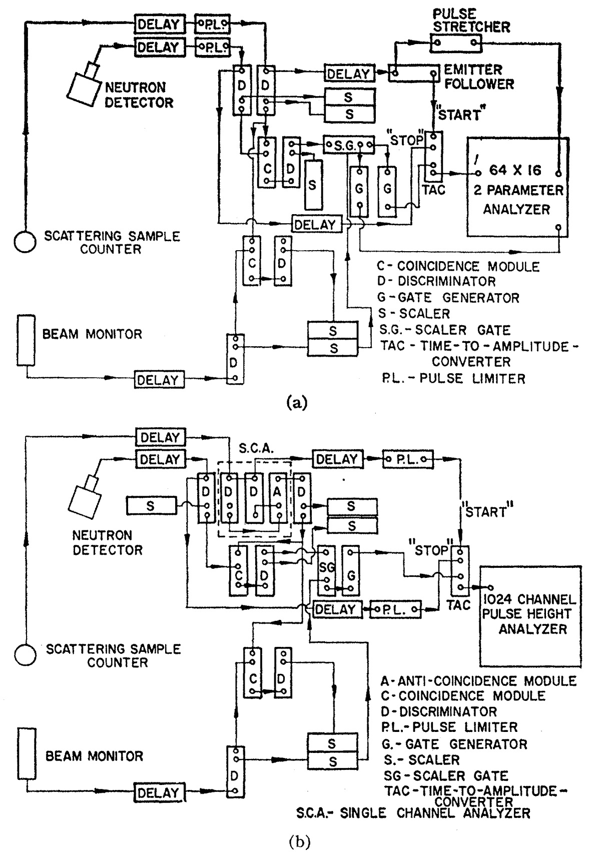

FIG. 4. (a) Block diagram of the electronics used to analyze both the neutron time of flight and the recoil pulse from the scattering sample in a two-dimensional pulse-height analyzer. (b) Block diagram of the electronics with one-dimensional analysis of the neutron time of flight and a single-channel analysis (SCA) of the recoil pulse height.

that the gain setting on the scattering-sample counter be varied to compensate for the kinematic variation of the recoil energy of the deuterons. These variations were made by changing the counter gain and leaving the appropriate discriminator thresholds fixed. All settings used the Na^{22} pulse-height spectrum as a reference.

The over-all time resolution of the system was checked periodically with a Co^{60} source. Figure 5 shows a typical time-of-flight spectrum obtained with this source of two simultaneously emitted γ rays. The full width at half-height is 2.5 nsec. Another method of checking the time-of-flight system was to perform a measurement using pulses from the α detector (beam monitor) and the scattering-sample counter to drive the logic circuits. Figure 6 is a plot of the resulting time-of-flight spectrum. It indicates a full width at half-maximum of 3.3 nsec so that from the large signal-to-background ratio one can conclude that the correlation between α counts and neutrons interacting in the scattering-sample counter is very high. The slight increase in the distribution width can be attributed to the energy spread of the recoil α particles mentioned above.

[11] C. B. Ward and C. M. York, Nucl. Instr. Methods **23**, 213 (1963); C. Ward, A. Berick, E. Tagliaferri, and C. York, *ibid.* **30**, 61 (1964).

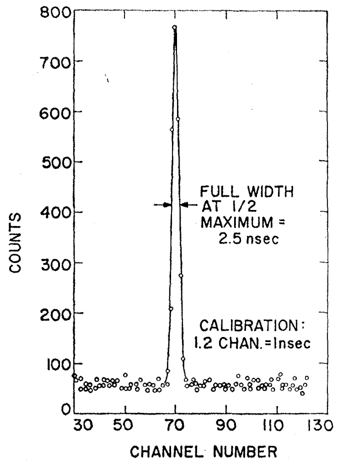

FIG. 5. Time-of-flight spectrum obtained as a calibration of the system by using the γ rays from Co^{60}.

IV. DATA

A. General Discussion

The experimental arrangement shown in Fig. 1, with the entire array of shielding surrounding the neutron source, was used for measurements taken at laboratory angles of 10° and at 5° intervals from 70° to 130°. However, for the remaining angles it was found sufficient to remove all of the shielding shown in the figure and to use only a steel bar to protect the neutron detector from those neutrons emitted directly toward it from the source.

Figure 7 is an example of a neutron time-of-flight spectrum taken at a laboratory angle of 25°, where one-dimensional analysis of the data was performed. The small peak on the left is due to Compton-scattered γ rays and the large one to the right is due to the elastically scattered neutrons. All of the pulse-height spectra showed a "low-energy tail" to the right of the neutron peak. This tail is significantly higher than the background events observed between the γ-ray and neutron peaks. Several possibilities were considered to explain this tail: low-energy incident neutrons originating in the tritium target; degraded neutrons originating in the shielding around the neutron source; neutrons scattered into the target from the floor, walls, ceiling, or air between the source and target; inscattered neutrons originating between the target and detector; multiple scattering in the target; inelastic scattering in the target; a characteristic of the time-to-amplitude converter; or a characteristic of the photomultiplier tubes. The conclusion which was drawn from this rather lengthy series of investigations was that the cause of the apparent "low-energy" tail to the right of the elastic peak could not be determined. With this problem in mind, the following method was used to extract the elastic scattering data from the time-of-flight spectra. First, the background level was determined by averaging the number of counts per channel in those channels lying between the neutron elastic peak and the γ-ray peak. Next, the number of counts under the neutron peak were summed from the point on the left where the peak begins to rise above background to the point on the right where the tail begins to break from the elastic peak. The background was then subtracted from this total. Several data runs were made at each scattering angle to test the self-consistency of this method and the system as a whole. The results proved to be quite consistent.

B. Corrections to the Data

Before the cross sections could be evaluated, several corrections had to be applied to the data. These corrections were:

1. Electronic Dead-Time Correction

The dead times of the various electronic components making up the counting system were determined with a 3-Mc/sec variable rate pulse generator or with the output of a 56 AVP phototube subjected to the activity of a strong γ-ray source. These tests resulted in a maximum correction of 2.0% for the two-parameter data. For the one-parameter data there was an over-all correction of 3.3% made at one point while the remaining corrections were less than 1.0%.

2. Correction for False Start of Stop Pulse

There is a finite probability that a valid start or stop pulse will be preceded by a pulse which is too small in amplitude to trigger the discriminator but large enough to trigger the time-to-amplitude converter. The data have not been corrected for this effect because an estimated upper limit of 0.2% can be placed on its magnitude.

3. Neutron Scattering on Carbon

There are three neutron-carbon reactions which fulfill the requirements of being energetically possible at 14 MeV and which also have a final-state free neutron. These are (i) the $C(n,n)C$ elastic scattering, (ii) the $C(n,n')3He^4-7.26$-MeV reaction, and (iii) the

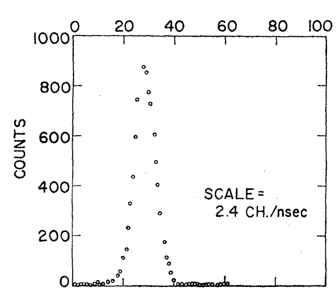

FIG. 6. Time-of-flight spectrum of the neutron beam obtained from the beam monitor and the scattering-sample counter.

$C(n,n')C^* \rightarrow C'+\gamma$ excitation reaction. The combination of time-of-flight requirements placed on the recoil particles in the scattering sample served to eliminate the contamination to the data from the first two reactions. There was, however, a small contribution to the data from the third reaction, $C(n,n')C^*$. Because the interaction probability of the decay γ rays from C^* is small in the scintillator, the corrections to the scattering data were shown to be less than 0.5%.

4. *Loss of Valid Events because of Recoils Interacting with the Wall of the Target*

If a valid proton or deuteron recoil particle collides with the wall of the target container before releasing an adequate quantity of scintillation energy, the event will not be recorded. Since all of the recorded events take place in a horizontal plane, interactions with the upper and lower surfaces of the container were neglected. The interaction with the cylindrical wall only occurs over one-half of the surface area, since the recoil particles are moving away from the wall on one side and towards it on the other. The correction consists of, first, determining the minimum range through which a recoil particle must travel in the scintillation medium in order to deposit enough energy to be detected. When this quantity has been determined for each of the angles at which data were taken, it is possible to determine how much of the target volume is not effective in producing valid events. The maximum corrections were made to the data obtained at the backward scattering angles where the recoils have the greatest amount of energy and range. Although the n-d corrections ranged from 0.01 to 4.5%, the maximum over-all correction applicable to relative n-d-versus-n-p response [cf. Eq. (3)] was found to be about 2.4%.

5. *Recoil Particles Reacting in the Scattering Sample*

If a recoil proton or deuteron reacts inelastically with one of the nuclei in the scattering sample, the loss of scintillation energy might be reduced so that the event would not be recorded. A detailed analysis of this phenomenon was not carried out because of insufficient cross-section data on the possible inelastic reactions in deuterated or nondeuterated benzene. However, it was possible to set an upper limit on the over-all magnitude of this correction by using the maximum cross sections found in the literature.[12] These data gave an upper limit to the over-all correction of $<0.2\%$.

6. *Hydrogen Contamination in the Deuterated Scattering Sample*

The amount of hydrogen contamination in the deuterated scattering sample was obtained from the chemical analysis supplied by the manufacturer.[10] The maximum correction to the data was 0.58%, but at most angles the correction was zero.

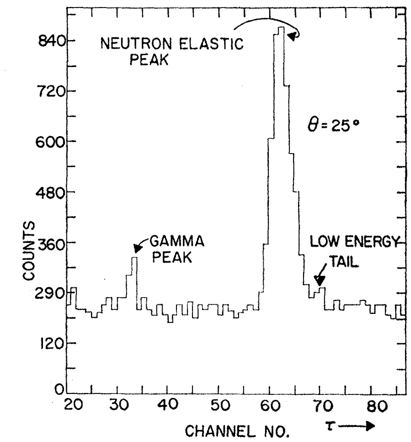

FIG. 7. A typical time-of-flight spectrum for scattered neutrons using one-dimensional analysis.

7. *Contribution from the $d(n,n'')n'p$ "Breakup" Reaction*

Because of the lack of sufficient data on the $d(n,n'')np'$ reaction, the experimentally determined cross sections for the $d(p,p'')np'$ mirror reaction[13] were used in the calculation. The fraction of events giving rise to valid pulse amplitudes in the scattering-sample scintillator was determined by assuming that the recoil-proton energy distribution was determined by phase-space considerations only. The maximum correction to the data was 3.0%, and the correction was negligible for laboratory scattering angles greater than 40°.

8. *Neutrons Multiply Scattered in the Scattering Sample*

The number of scattered neutron events in which the neutrons underwent more than one interaction in the scattering sample was determined through the use of a multiple-scattering program called MAGGIE.[14] The details of the calculation, when applied to this experiment, are given elsewhere.[8] The inscattering correction was a 1.0 to 4.69% effect for the n-p part of the experiment and a 1.25 to 6.5% effect for the n-d portion.

The determination of the fraction of valid events lost because of multiple scattering was straightforward. The assumption was made that any scattered neutron directed toward the detector would be scattered away from it in undergoing any further interactions and be lost. It was determined that this assumption was in error by no more than 0.2%. The calculation was carried out in detail by determining the fractional loss

[12] S. Mayo, W. Schimmerling, M. J. Sametband, and R. M. Eisberg, Nucl. Phys. **62**, 393 (1965); J. E. A. Lys and L. Lyons, *ibid.* **74**, 261 (1965).

[13] S. Kikuchi, J. Sanada, S. Suwa, I. Hayashi, K. Nisimura, and K. Fukunaga, J. Phys. Soc. Japan **15**, 749 (1960).

[14] J. B. Parker, J. H. Towle, D. Sams, W. B. Gilboy, A. D. Purnell, and H. J. Stevens, Nucl. Instr. Methods **30**, 77 (1964).

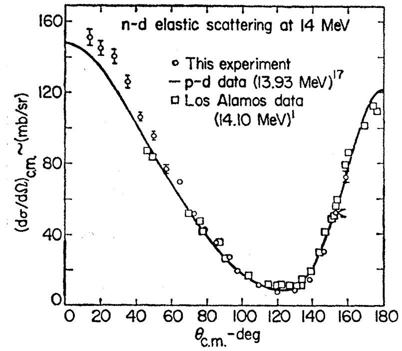

FIG. 8. A plot of the final results of this experiment together with results on other n-d (Ref. 1), as well as p-d experiments (Ref. 17).

from each differential element of volume in the target and integrating over the target volume. Although the magnitude of the correction varied from 18 to 43%, it is the difference in the correction for the n-d and corresponding n-p data which enters in the determination of final cross-section values [see Eq. (3)]. This difference varied between 0.4 and 6.7%.

9. *Accuracy of the Corrections*

For purposes of assigning probable errors to the corrected data, it was assumed that the corrections for the electronic dead times and total absorption cross sections[15] were known to 10% accuracy while a uniform 20% error was assigned to the remaining corrections.

V. RESULTS

The corrected results are presented in Table I. Absolute values of the cross section were obtained by assuming that the angular distribution for n-p scattering is of the form[1] $(1+a\cos^2\theta^*)$. The total cross section at 14.10 MeV was taken to be 689±5 mb[9] and was corrected to 14.3 MeV with the relation $\sigma=4.83\sqrt{E}-0.578$ b.[16] The value of a in the angular distribution was 0.048±0.028. The probable errors listed for the cross sections reflect uncertainty in the n-p angular distribution. The angular widths given in Table I represent the full widths at half-maximum of the angular resolution functions for each detector position. In calculating the angular resolution functions the detailed geometries of both scattering sample and detector were considered together with the beam attenuation in the scattering sample and the variation of the scattering cross section with angle. In most cases the mean scattering angle and most probable scattering angle were not identical. The mean scattering angles are listed in Table I.

TABLE I. n-d elastic scattering at 14.3 MeV.

$\bar{\theta}_{\rm lab}$ (deg)	$\sigma(\theta)$ (mb/sr)	$\bar{\Psi}_{\rm c.m.}$ (deg)	$\sigma(\Psi)$ (mb/sr)
9.03±1.7	332.5±11.6	13.5±2.6	149.2±5.3
13.6 ±1.8	315.2±10.5	20.4±2.7	143.1±4.8
18.6 ±1.8	294.2± 9.6	27.8±2.6	138.6±4.5
23.7 ±1.8	262.4± 8.8	35.3±2.6	124.4±4.5
28.6 ±1.8	214.2± 6.5	42.4±2.6	104.7±3.2
33.7 ±1.8	185.6± 5.6	49.8±2.6	94.1±2.9
38.7 ±1.8	143.6± 4.5	57.0±2.5	76.0±2.4
43.8 ±1.8	123.0± 3.7	64.2±2.4	68.4±2.0
48.9 ±1.8	87.2± 2.6	72.3±2.4	51.3±1.5
53.9 ±1.8	67.2± 2.2	77.9±2.3	42.1±1.4
58.9 ±1.8	49.9± 1.7	84.5±2.3	33.4±1.1
64.0 ±1.7	37.4± 1.4	92.1±2.2	26.8±1.0
69.4 ±1.7	24.8± 0.8	97.1±2.0	19.6±0.6
79.5 ±1.8	12.6± 0.4	108.9±1.9	11.9±0.4
89.7 ±1.7	7.0± 0.2	119.8±1.7	8.0±0.3
99.8 ±1.7	6.2± 0.2	129.2±1.6	8.8±0.3
109.9 ±1.8	8.3± 0.4	138.1±1.4	14.5±0.7
119.9 ±1.8	14.2± 0.6	145.6±1.3	30.2±1.2
130.0 ±1.8	20.2± 0.8	152.5±1.2	51.4±2.1

Table II lists the salient features of the present investigation together with some previous n-d elastic scattering experiments reported in the literature for comparison. The n-d results from Ref. 1, as well as a curve fitted to the p-d results[17] at 13.93 MeV, are presented in Fig. 8 together with the data from this experiment. The comparison shows that the present data are higher in the forward angles, lower around the minimum, and show general agreement in the backward angular region.

The data were fitted to a Legendre polynomial in $\cos\theta_{\rm c.m.}$, the best least-squares fit being obtained from an eighth-order polynomial. Table III lists the coefficients for the fit. The χ^2 "goodness-of-fit" test gives a 20% probability of obtaining a greater degree of dispersion of the data points. The angular distribution was integrated to obtain a value of the total n-d elastic cross section at 14.3 MeV of 650±6 mb. This is to be compared with the results of Ref. 1 of 670±100 and 610±30 mb.

Attempts to fit the data of this experiment to theoretical curves of the type calculated by Aaron *et al.*[18] were completely inadequate. These models invariably fail to include a sufficient contribution from states of high angular momentum to produce the large amount of scattering in the forward direction which has been observed in this experiment.

VI. SUMMARY AND CONCLUSIONS

The angular distribution of 14.3-MeV neutrons elastically scattered from deuterons was measured by combining a neutron time-of-flight measurement with an energy determination of the recoil deuterons. The

[15] Robert J. Howerton, University of California Radiation Laboratory Report No. UCRL-5226, Part I, 1959 (unpublished).

[16] Nuclear Data Tables, Nuclear Reaction Graphs, Part 3 (unpublished).

[17] S. Kikuchi, J. Sanada, I. Hayashi, K. Nisimura, and K. Fukunaga, J. Phys. Soc. Japan **15**, 9 (1960). The fit to the purely nuclear part of the interaction was done by Dr. W. T. H. Van Oers of the Physics Department of UCLA (private communication, 1967).

[18] R. Aaron, R. D. Amado, and Y. Y. Yam, Phys. Rev. **140**, B1291 (1965).

TABLE II. *n-d* elastic scattering experiments done in the 14.0-MeV region. Comparison of the present investigation with previous investigations.

Authors	Year	Method	Angular range (c.m.)	Angular resol. (lab)	Statistical accuracy (%)	E_n (MeV)
Coon and Taschek[a]	1949	Detect recoil deuteron in counter telescope.	70°–180° (7 angles)	±7°	±10	14.1
Griffith, Remley, and Kruger[b]	1950	Detect deuteron in cloud chamber with CD_4 and CD_3H gases.	50°–170° (7 angles)	±5°	±(3.2–7)	12.5
T. C. Griffith[c]	1952	Detect recoil deuteron in photographic emulsion.	70°–155° (7 angles)	±(3°–4°)	±(8–14)	13.9
Allred, Armstrong, and Rosen[d]	1953	Detect recoil deuteron in photographic emulsion.	46°–176° (26 angles)	±(2.5°–5°)	±(3.4–12)	14.1
Seagrave[d]	1954	Recoil counter telescope to detect deuteron. 2 dE/dx counters for particle identification.	70°–174° (8 angles)	±(4°–7°)	±(1.5–10)	14.1
Berick *et al.*	1966	Detect recoil deuteron and scattered neutron. 2*D* analyser or single-channel analyser on recoils.	13.5°–158.6° (20 angles)	±1.8°	±(2–3)	14.3

[a] J. H. Coon and R. F. Taschek, Phys. Rev. **76**, 710 (1949).
[b] G. L. Griffith, M. E. Remley, and P. G. Kruger, Phys. Rev. **79**, 443 (1950).
[c] T. C. Griffith, Proc. Phys. Soc. (London) **A66**, 894 (1953).
[d] Reference 1.

measurements covered the forward angular scattering region which had not been covered by previous experiments. Both the angular resolution and the statistical accuracy of the measurements are superior to previous experiments performed with neutrons in this energy region. In addition, the range of measured scattering angles has been considerably extended by the present investigation.

The cross-section values were obtained by comparing each *n-d* measurement to a corresponding *n-p* measurement in which the scattered-neutron energies were approximately equal. This comparison technique minimized the magnitudes of the corrections made to the data and the uncertainties arising from those corrections. The angular distribution obtained from this investigation shows higher probabilities for scattering into the forward and backward angular regions and a lower probability for the central region around the minimum when compared with those of previous experiments. This indicates an enhancement of the contribution to the scattering amplitude made by higher-order partial waves, and an eighth-order polynomial was required to obtain a best fit to the data, indicating an appreciable *g*-wave contribution to the scattering amplitude. The value of the total cross section obtained from these data was found to be in satisfactory agreement with previous measurements.

TABLE III. Angular distribution for neutron-deuteron elastic scattering at 14.3 MeV.

Coefficients for the Legendre polynomial fit in terms of $\text{cosine}_{\text{c.m.}}$ (mb/sr).	
a_0	51.6±0.5
a_1	52.5±1.2
a_2	60.4±1.5
a_3	−19.5±1.8
a_4	21.2±2.1
a_5	−15.0±2.2
a_6	7.5±2.5
a_7	−5.5±1.9
a_8	1.2±1.9

ACKNOWLEDGMENTS

The authors wish to express their appreciation to Dr. H. K. Ticho, W. T. H. van Oers, and C. B. Ward of UCLA and Dr. J. D. Seagrave of the Los Alamos Scientific Laboratory for their important contributions to this work. Valuable assistance in taking the data was rendered by D. Berk, J. Berk, C. McDowell, and M. Monti, while R. Nordberg was essential in maintaining and operating the Van de Graaff accelerator.